

# Texture segmentation via a diffusion-segmentation scheme in the Gabor feature space

Chen Sagiv, Nir A. Sochen, Yehoshua. Y. Zeevi

*Abstract*— We address the problem of texture segmentation in the context of the Gabor feature space of images. Gabor filters which are tuned to different orientations, scales and frequencies are applied to textured images to create the Gabor feature space. We regard the scale, orientation and frequency for which maximum response of the Gabor filters was obtained. A two-dimensional Riemannian manifold of local features is extracted via the Beltrami framework. The metric of this surface is a good indicator of texture changes and is used, therefore, in a Beltrami based diffusion mechanism and in a geodesic active contours algorithm for texture segmentation. The innovation of this work lies in using the metric of the feature manifold which integrates information from all the features, in both the diffusion and segmentation processes.

*Keywords*— Texture, Texture segmentation, Gabor analysis, Geometric-based algorithms, Geodesic active contours, Beltrami framework, Anisotropic diffusion, image manifolds.

## I. INTRODUCTION

THE task of discriminating between different textures is not a difficult one for the human observer. However, when it comes to image processing and computer vision, this task is far from being an easy one, as real world textures are difficult to mathematically model and analyze. Among the approaches to the analysis of textures are local geometric primitives [7], local statistical features [2], random field models [6], [3] and the FRAME theory [23]. We address the problem of texture segmentation in the context of the Gabor feature space of images.

The motivation for the use of Gabor filters in texture analysis is double fold. First, it is believed that simple cells in the visual cortex can be modeled by Gabor functions [13], [4], and that the Gabor scheme provides a suitable representation for visual information in the combined frequency-position space [15]. Second, the Gabor representation has been shown to be optimal in the sense of minimizing the joint two-dimensional uncertainty in the combined spatial-frequency space [5].

A great deal of attention has been devoted in recent years to the "snakes", or active contour models, which were proposed by Kaas et al [8] for intensity based image segmentation. In this framework an initial contour is deformed towards the boundary of an object to be detected. The evolution equation is derived from minimization of an energy functional, which obtains a minimum for a curve located

at the boundary of the object. The geodesic active contours model [1], [9] offers a different perspective for solving the boundary detection problem; It is based on the observation that the energy minimization problem is equivalent to finding a geodesic curve in a Riemannian space whose metric is derived from image contents. The geodesic curve can be found via a *parameterization invariant* geometric flow. Utilization of the Osher and Sethian level set numerical algorithm [16] allows automatic handling of changes of topology.

This snakes model was extended to the vector valued active contours to handle more complex scenery such as color images [20] and multi-texture images. Some recent related work includes the one of Paragios and Deriche [14] who generate the image's texture feature space by filtering the image using Gabor filters. Texture information is then expressed using statistical measurements, and segmentation is achieved by application of geodesic snakes to the statistical feature space. Shah [21] develops and applies curve evolution and segmentation algorithms where anisotropic metrics are considered. Lorigo et al [12] used both image intensity and its variance for MRI images' segmentation.

The Gaborian spatial-feature space can be described, via the Beltrami framework [22], as a  $4D$  Riemannian manifold [10] embedded in  $\mathbf{R}^6$ . Based on this approach, the intensity based geodesic active contours method was generalized to the Gabor-feature space of images, where at each pixel the features that yielded the maximum response for the Gabor filters, are selected [19]. The metric introduced in the Gabor space was used to derive the inverse edge indicator function  $E$ , which attracts in turn the evolving curve towards the boundary in the geodesic snakes scheme. Using this approach the geodesic snakes yields good results when the textures are homogeneous and can be characterized by these maximum values.

However, the maximum values provide only partial information regarding image structure in the full Gabor feature space. This may, in turn, generate less than satisfactory results in case of more complex textures. One solution to this problem is to apply the geodesic snakes mechanism to the complete Gabor feature space and interpret the Gabor transform of an image as a function assigning for each pixel's coordinates, scale, orientation and frequency, a value. Thus, the Gabor transform of an image may be viewed as a  $5D$  manifold embedded in  $\mathbf{R}^7$ . An alternative solution is to improve the results obtained from the  $2D$  manifold embedded in  $7D$  space approach. In a previous study [18], a single Gabor feature, the orientation, was smoothed using the weighted area minimization method prior to using it in the geodesic

C. Sagiv and N. Sochen are with the Department of Applied Mathematics, University of Tel Aviv, Ramat-Aviv, Tel-Aviv 69978, Israel. E-mail: chensagi,sochen@post.tau.ac.il. Y.Y. Zeevi is with the Department of Electrical engineering, Technion - Israel Institute of Technology, Technion City, Haifa 32000, Israel, Email: zeevi@ee.technion.ac.il

snakes mechanism. In this study we evaluate the impact of coupling information from several Gabor features into a single diffusion-segmentation scheme to achieve better results comparing to the same procedure applied to each of the features separately. We use Gabor filters which are tuned to different orientations, scales and sine grating frequencies. These are applied to textured images to create the Gabor feature space. The scale, orientation and frequency for which maximum response of the Gabor filters was obtained are considered. The features are presented, via the Beltrami framework, as a Riemannian manifold with local coordinates  $(x, y)$  embedded in  $\mathbf{R}^7$ , or explicitly  $(x, y, R(x, y), J(x, y), \sigma(x, y), \theta(x, y), f(x, y), )$ , where  $R$  and  $J$  are the real and imaginary parts of the Gabor transformed image, and  $\theta$ ,  $\sigma$  and  $f$  are the direction, scale and frequency for which a maximal response has been achieved. We use the Beltrami flow for denoising the Gabor features. Next, the denoised features are used to obtain a noise free metric of the Gabor feature manifold which is used as an inverse edge detector in the geodesic snakes mechanism.

Thus, the innovation of this study lies in using a metric which integrates information from all features, rather than one, in both the diffusion and segmentation phases.

This paper is organized as follows: In section 2 we describe the geodesic active contours method for intensity images. Next, in section 3 we describe the generation of the Gabor feature space. In section 4 we show how to apply the geodesic snakes mechanism in the Gabor feature space. Finally in section 5, we provide some preliminary results.

## II. GEODESIC ACTIVE CONTOURS

In this section we review the geodesic active contours method for non-textured images [1], [9]. The generalization of the technique for texture segmentation is described in section 4.

Let  $\mathbf{C}(\mathbf{q}) : [0, 1] \rightarrow \mathbf{R}^2$  be a parametrized curve, and let  $I : [0, a] \times [0, b] \rightarrow \mathbf{R}^+$  be the given image. Let  $E(r) : [0, \infty[ \rightarrow \mathbf{R}^+$  be an inverse edge detector, so that  $E$  approaches zero when  $r$  approaches infinity. Visually,  $E$  should represent the edges in the image. Minimizing the energy functional proposed in the classical snakes is generalized to finding a geodesic curve in a Riemannian space by minimizing:

$$L_R = \int E(|\nabla I(\mathbf{C}(q))|) |\mathbf{C}'(q)| dq. \quad (1)$$

We may see this term as a weighted length of a curve, where the Euclidean length element is weighted by  $E(|\nabla I(\mathbf{C}(q))|)$ . The latter contains information regarding the boundaries within the image. The resultant evolution equation is the gradient descent flow:

$$\frac{\partial \mathbf{C}(t)}{\partial t} = E(|\nabla I|) k \mathbf{N} - (\nabla E \cdot \mathbf{N}) \mathbf{N}, \quad (2)$$

where  $k$  denotes curvature.

If we now define a function  $U$ , so that  $\mathbf{C} = ((x, y) | U(x, y) = 0)$ , we may use the Osher-Sethian Level-

Sets approach [16] and replace the evolution equation for the curve  $\mathbf{C}$ , with an evolution equation for the embedding function  $U$ :

$$\frac{\partial U(t)}{\partial t} = |\nabla U| \text{Div} \left( E(|\nabla I|) \frac{\nabla U}{|\nabla U|} \right). \quad (3)$$

A popular choice for the stopping function  $E(|\nabla I|)$  is given by:

$$E(|\nabla I|) = \frac{1}{1 + |\nabla I|^2},$$

however, other image-specific functions may be used.

## III. FEATURE SPACE AND GABOR TRANSFORM

The Gabor scheme and Gabor filters have been studied by numerous researchers in the context of image representation, texture segmentation and image retrieval. A Gabor filter centered at the 2D frequency coordinates  $(U, V)$  has the general form of:

$$h(x, y) = g(x', y') \exp(2\pi i(Ux + Vy)) \quad (4)$$

where

$$(x', y') = (x \cos(\phi) + y \sin(\phi), -x \sin(\phi) + y \cos(\phi)), \quad (5)$$

$$g(x, y) = \frac{1}{2\pi\sigma^2} \exp\left(-\frac{x^2}{2\lambda^2\sigma^2} - \frac{y^2}{2\sigma^2}\right), \quad (6)$$

$\lambda$  is the aspect ratio between  $x$  and  $y$  scales,  $\sigma$  is the scale parameter, and the major axis of the Gaussian is oriented at angle  $\phi$  relative to the  $x$ -axis and to the modulating sinewave gratings.

Accordingly, the Fourier transform of the Gabor function is:

$$H(u, v) = \exp\left(-2\pi^2\sigma^2((u' - U')^2\lambda^2 + (v' - V')^2)\right) \quad (7)$$

where,  $(u', v')$  and  $(U', V')$  are rotated frequency coordinates. Thus,  $H(u, v)$  is a bandpass Gaussian with its minor axis oriented at angle  $\phi$  from the  $u$ -axis, and the radial center frequency  $f$  is defined by :  $f = \sqrt{U^2 + V^2}$ , with orientation  $\theta = \arctan(V/U)$ . Since maximal resolution in orientation is desirable, the filters whose sinewave gratings are cooriented with the major axis of the modulating Gaussian are usually considered ( $\phi = \theta$  and  $\lambda > 1$ ), and the Gabor filter is reduced to:  $h(x, y, f) = g(x', y') \exp(2\pi i f x')$ .

It is possible to generate Gabor-Morlet wavelets from a single mother-Gabor-wavelet by transformations such as: translations, rotations and dilations. We also use different frequency values and generate, in this way, a set of filters for a known number of scales,  $S$ , orientations  $K$  and frequencies  $F$ . We obtain the following filters for a discrete subset of transformations:  $h_{lmn}(x, y) = a^{-m} h(\frac{x'}{a^m}, \frac{y'}{a^m}, f_l)$ , where  $(x', y')$  are the spatial coordinates rotated by  $\frac{\pi n}{K}$ ,  $m = 0 \dots S - 1$  and  $f_l$  is the frequency.

The feature space of an image is obtained by the inner product of this set of Gabor filters with the image:

$$W_{lmn}(x, y) = R_{lmn}(x, y) + iJ_{lmn}(x, y) = I(x, y) * h_{lmn}(x, y). \quad (8)$$

#### IV. APPLICATION OF GEODESIC SNAKES TO THE GABORIAN FEATURE SPACE OF IMAGES

The geodesic snakes mechanism is applied in the Gabor spatial feature space of images by generalizing the inverse edge indicator function  $E$ , which attracts in turn the evolving curve towards the boundary. A special feature of our approach is the metric introduced in the Gabor space, and used as the building block for the stopping function  $E$  in the geodesic active contours scheme.

It has already been suggested to view images and image feature space as Riemannian manifolds embedded in a higher dimensional space [22]. For example, a gray scale image is a 2D Riemannian manifold, with  $(x, y)$  as local coordinates, embedded in  $\mathbf{R}^3$  with  $(X, Y, Z)$  as local coordinates. The embedding map is  $(X = x, Y = y, Z = I(x, y))$ , and we write it, by abuse of notations, as  $(x, y, I)$ . When we consider feature spaces of images, e.g. color space, statistical moments space, and the Gaborian space, we may view the image-feature information as a  $N$ -dimensional manifold embedded in a  $N + M$  dimensional space, where  $N$  stands for the number of local parameters needed to index the space of interest and  $M$  is the number of feature coordinates. For example, we may view the Gabor transformed image as a 2D manifold with local coordinates  $(x, y)$  embedded in a 7D feature space. The embedding map is  $(x, y, R(x, y), J(x, y)\theta(x, y), \sigma(x, y), f(x, y))$ , where  $R$  and  $J$  are the real and imaginary parts of the Gabor transformed image, and  $\theta$ ,  $\sigma$  and  $f$  are the direction, scale and frequency for which a maximal response has been achieved.

A basic concept in the context of Riemannian manifolds is distance. Consider a two-dimensional manifold  $\Sigma$  with local coordinates  $(\sigma_1, \sigma_2)$ . Since the local coordinates are curvilinear, the distance is calculated using a positive definite symmetric bilinear form called the metric whose components are denoted by  $g_{\mu\nu}(\sigma_1, \sigma_2)$ :

$$ds^2 = g_{\mu\nu}d\sigma^\mu d\sigma^\nu, \quad (9)$$

where we used the Einstein summation convention : elements with identical superscripts and subscripts are summed over.

The metric on the image manifold is derived using a procedure known as pullback. The manifold's metric is then used for various geometrical flows. We shortly review the pullback mechanism. More detailed information can be found in [22].

Let  $X : \Sigma \rightarrow M$  be an embedding of  $\Sigma$  in  $M$ , where  $M$  is a Riemannian manifold with a metric  $h_{ij}$  and  $\Sigma$  is another Riemannian manifold. We can use the knowledge of the metric on  $M$  and the map  $X$  to construct the metric on  $\Sigma$ . This pullback procedure is as follows:

$$(g_{\mu\nu})_\Sigma(\sigma^1, \sigma^2) = h_{ij}(X(\sigma^1, \sigma^2)) \frac{\partial X^i}{\partial \sigma^\mu} \frac{\partial X^j}{\partial \sigma^\nu}, \quad (10)$$

where we used the Einstein summation convention,  $i, j = 1, \dots, \dim(M)$ , and  $\sigma^1, \sigma^2$  are the local coordinates on the manifold  $\Sigma$ .

If we pull back the metric of a 2D image manifold from the Euclidean embedding space  $(x, y, I)$  we get:

$$(g_{\mu\nu}(x, y)) = \begin{pmatrix} 1 + I_x^2 & I_x I_y \\ I_x I_y & 1 + I_y^2 \end{pmatrix}. \quad (11)$$

The determinant of  $g_{\mu\nu}$  yields the expression :  $1 + I_x^2 + I_y^2$ . Thus, we can rewrite the expression for the stopping term  $E$  in the geodesic snakes mechanism as follows:

$$E(|\nabla I|) = \frac{1}{1 + |\nabla I|^2} = \frac{1}{\det(g_{\mu\nu})}.$$

We may interpret the Gabor transform of an image as a function assigning to each pixel's coordinates, scale, orientation and frequency, a value ( $W$ ). Next, we get the scale, orientation and frequency for which we have received the maximum amplitude of the transform for each pixel. Thus, for each pixel, we obtain:  $W_{max}$ , the maximum value of the transform,  $\theta_{max}$ ,  $\sigma_{max}$  and  $f_{max}$  – the orientation, scale and frequency that yielded this maximum value. This approach results in a 2D manifold (with local coordinates  $(x, y)$ ) embedded in a 7D space (with local coordinates  $(x, y, R(x, y), J(x, y), \theta(x, y), \sigma(x, y), f(x, y))$ ). If we use the pullback mechanism described above we get the following metric:

$$g_{\mu\nu} = \begin{pmatrix} 1 + \sum w_i a(i)_x^2 & \sum w_i a(i)_x a(i)_y \\ \sum w_i a(i)_x a(i)_y & 1 + \sum w_i a(i)_y^2 \end{pmatrix}, \quad (12)$$

where  $i$  indexes the relevant Gabor features  $a(i)$ , and  $w_i$  accounts for the different scales of each Gabor feature. We use the fact that the determinant of the metric is a positive definite edge indicator to determine  $E$  as the inverse of the determinant of  $g_{\mu\nu}$  (see [17] for a similar use in color).

#### V. SMOOTHING THE GABOR FEATURE SPACE USING THE BELTRAMI FLOW

In the previous section we have described how the Gabor feature space can be treated as a 2D manifold embedded in 7D space. We have used a maximum criterion to obtain a single orientation, scale and frequency for each pixel location. However, this information does not always well represent the textural information and is sensitive to local variations in the texture characteristics. Therefore, the resultant Gabor features can be quite noisy. Also, some random noise can deteriorate the resultant data. Our aim is to reduce the amount of noise in the Gaborian features and obtain a smoother function to be used in the geodesic snakes mechanism. Denoising may be applied to each Gaborian feature separately, as was already shown in [18]. In this study we explore the possibility of coupling information from several Gabor features into a single diffusion scheme and to achieve better diffusion results comparing to the same procedure applied to each of the features, scale, orientation or frequency separately.

We define an energy functional which minimizes an area element,  $\sqrt{g}dx dy$ , of the features manifold

$$\mathbf{S}(x, y, R, J, \sigma, \theta, f) = \int \sqrt{g(a(i)_x, a(i)_y)} dx dy \quad (13)$$

where  $g$  is the determinant of the metric of the Gabor feature manifold, which is given in general for any number of features,  $a(i)$  - in this case  $(x, y, R(x, y), J(x, y), \theta(x, y), \sigma(x, y), f(x, y))$  - each weighted by  $w_i$  by equation 12.

The combination  $\sqrt{g}dx dy$ , an area element of the Gabor features manifold, is the term that forces smoothing as the features field reduces its overall area when it flows towards the optimal solution. The resultant gradient descent process is the Beltrami flow for each Gaborian feature. Let  $a$  represent one of the Gaborian features, then according to the Euler-Lagrange method:

$$\frac{\delta S}{\delta a} = -div \left( \frac{\nabla_a(g)}{2\sqrt{g}} \right), \quad (14)$$

where

$$\nabla_a(g) = \left( \frac{\partial g}{\partial a_x}, \frac{\partial g}{\partial a_y} \right). \quad (15)$$

According to the steepest descent method the evolution equations are:

$$a_t = -\frac{1}{\sqrt{g}} \frac{\delta S}{\delta a}. \quad (16)$$

We obtain a set of coupled evolution equations. The update of the values of  $R, J, \sigma, \theta, f$  is done at the end of each iteration.

## VI. RESULTS AND DISCUSSION

We use the Beltrami flow to smooth the Gaborian features  $(R, J, \theta, \sigma, f)$  which are treated as a  $2D$  manifold  $(x, y)$  embedded in  $7D$  Euclidean space,  $(x, y, R, J, \theta, \sigma, f)$ . Following the denoising phase, we can use  $(R(x, y), J(x, y), \theta(x, y), \sigma(x, y), f(x, y))$  as the input to the geodesic snakes algorithm. Geodesic snakes is an efficient geometric flow scheme for boundary detection, where the initial conditions include an arbitrary function  $U$  which implicitly represents the curve, and a stopping term  $E$  which contains the information regarding the boundaries in the image. We generalize the definition of gradients, usually considered in the context of intensity gradients over  $(x, y)$  to other possible gradients in scale, orientation and frequency. This gradient information is the input function  $E$  to the newly generalized geodesic snakes flow.

In the example the test image is of a zebra (figure 1). The resultant boundary when all the Gabor features are taken into account (figure 2) is better than the boundary obtained when only the orientation information is used (figure 3). This is because each Gabor component, scale, orientation or frequency captures another part of the boundary to be detected. Diffusing all the Gabor features using the metric of the 7-dimensional manifold, results in a enhancing boundaries which are manifested in several Gabor features and attenuating boundaries which are present in only one or only a few Gabor features.

As can be seen, using the metric when all features are considered leads to better segmentation results than the one obtained when the metric used depends on one parameter only. Currently, we apply the porcupine approach

suggested in [11] in order to obtain a more robust orientation diffusion.

## REFERENCES

- [1] V. Caselles and R. Kimmel and G. Sapiro, "Geodesic Active Contours", *International Journal of Computer Vision*, 22(1), 1997, 61-97.
- [2] R. Conners and C. Harlow "A Theoretical Comparison of Texture Algorithms" *IEEE Transactions on PAMI*, 2, 1980, 204-222.
- [3] G.R. Cross and A.K. Jain, "Markov Random Field Texture Models" *IEEE Transactions on PAMI*, 5, 1983, 25-39.
- [4] J.G. Daugman, "Uncertainty relation for resolution in space, spatial frequency, and orientation optimized by two-dimensional visual cortical filters", *J. Opt. Soc. Amer.* 2(7), 1985, 1160-1169.
- [5] D. Gabor "Theory of communication" *J. IEEE*, 93, 1946, 429-459.
- [6] S. Geman and D. Geman "Stochastic relaxation, Gibbs distribution and the Bayesian restoration of images", *IEEE Transactions on PAMI*, 6, 1984, 721-741.
- [7] B. Julesz "Texton Gradients: The Texton Theory Revisited", *Biol Cybern*, 54, (1986) 245-251.
- [8] M. Kaas, A. Witkin and D. Terzopoulos, "Snakes : Active Contour Models", *International Journal of Computer Vision*, 1, 1988, 321-331.
- [9] S. Kichenassamy, A. Kumar, P. Olver, A. Tannenbaum and A. Yezzi, "Gradient Flows and Geometric Active Contour Models", *Proceedings ICCV'95*, Boston, Massachusetts, 1995, 810-815.
- [10] R. Kimmel, N. Sochen and R. Malladi, "On the geometry of texture", *Proceedings of the 4th International conference on Mathematical Methods for Curves and Surfaces*, St. Malo, 1999. Report, Berkeley Labs. UC, LBNL-39640, UC-405, November, 1996.
- [11] R. Kimmel and N. Sochen. "Orientation Diffusion or How to Comb a Porcupine ? ", Special issue on PDEs in Image Processing, Computer Vision, and Computer Graphics, *Journal of Visual Communication and Image Representation*. In press.
- [12] L.M. Lorigo, O. Faugeras, W.E.L. Grimson, R. Keriven, R. Kikinis, "Segmentation of Bone in Clinical Knee MRI Using Texture-Based Geodesic Active Contours", *Medical Image Computing and Computer-Assisted Intervention*, 1998, Cambridge, MA, USA.
- [13] S. Marcelja, "Mathematical description of the response of simple cortical cells", *J. Opt. Soc. Amer.*, 70, 1980, 1297-1300.
- [14] N. Paragios and R. Deriche, "Geodesic Active Regions for Supervised Texture Segmentation", *Proceedings of International Conference on Computer Vision*, 1999, 22-25.
- [15] M. Porat and Y.Y. Zeevi, "The generalized Gabor scheme of image representation in biological and machine vision", *IEEE Transactions on PAMI*, 10(4), 1988, 452-468.
- [16] S.J. Osher and J.A. Sethian, "Fronts propagating with curvature dependent speed: Algorithms based on Hamilton-Jacobi formulations", *J of Computational Physics*, 79, 1988, 12-49.
- [17] R. Goldenberg, R. Kimmel, E. Rivlin, M. Rudzsky: Fast Geodesic Active Contours, *IEEE Tran. on Image Processing*, 10(10):1467-75, 2001.
- [18] C. Sagiv, N.A. Sochen, Y.Y. Zeevi, "Gabor Feature Space Diffusion via the Minimal Weighted Area Method", M. Figueiredo, J. Zerubia, A.K. Jain (Eds.), *Proceedings of Energy Minimization Methods in Computer Vision and Pattern Recognition, Lecture Notes in Computer Science* Vol. 2134, Springer, Berlin, 621-635, 2001.
- [19] C. Sagiv, N. Sochen, and Y.Y. Zeevi, "Gabor Space Geodesic Active Contours", G. Sommer, Y.Y. Zeevi (Eds.), *Algebraic Frames for the Perception-Action Cycle, Lecture Notes in Computer Science*, Vol. 1888, Springer, Berlin, 2000.
- [20] G. Sapiro, "Vector Valued Active Contours", *Proc. IEEE Conference on Computer Vision and Pattern Recognition*, 680-685, 1996.
- [21] J. Shah, "Riemannian Drums, Anisotropic Curve Evolution and Segmentation", *Proceedings of Scale-Space 1999.*, Eds. Nielsen, P. Johansen, O.F. Olsen, J. Weickert, Springer, 129-140.
- [22] N. Sochen, R. Kimmel and R. Malladi, "A general framework for low level vision", *IEEE Trans. on Image Processing*, 7, (1998) 310-318.
- [23] S.C. Zhu, Y.N. Wu and D.B. Mumford, "Equivalence of Julesz ensembles and FRAME models", *International Journal of Computer Vision*, 38(3), 2000, 247-265.



Fig. 1. The original image is of a zebra.

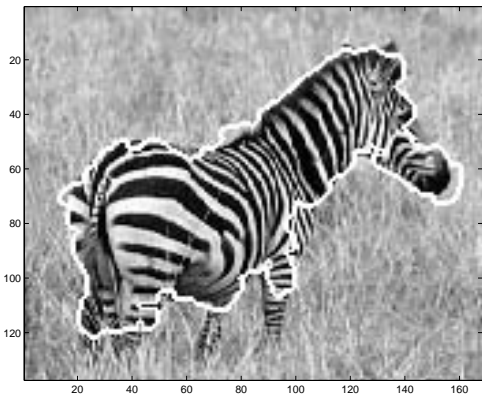


Fig. 2. The resultant boundary when the gradient information from all Gabor features is integrated.



Fig. 3. The resultant boundary when only the information from the orientation feature is accounted for.